forests

MDPI

Article

Genetic, Phenotypic, and Pathogenic Variation in *Phytophthora pseudosyringae:* Implications for Larch Dieback in Britain

Anna R. Harris [1,*], Martin S. Mullett [2] and Joan F. Webber [1]

[1] Pathology Department, Forest Research, Alice Holt Lodge, Farnham, Surrey GU10 4LH, UK; joan.webber@forestresearch.gov.uk
[2] Department of Forest Protection and Wildlife Management, Mendel University in Brno, 613 00 Brno, Czech Republic; martin.mullett@mendelu.cz
* Correspondence: anna.harris@forestresearch.gov.uk

Abstract

The oomycete *Phytophthora pseudosyringae* is mainly associated with rhizosphere infections of declining oak, beech, and alder in mainland Europe where it is considered native. However, the species has recently come to prominence in Britain, initially by causing significant damage to the heathland and woodland dwarf shrub *Vaccinium myrtillus*, then more recently associated with aerial infections on larch (*Larix*). The emergence of *P. pseudosyringae* on conifers raises concerns for forestry, particularly of larch in Europe, plus questions about its significance compared to *P. ramorum*, which has killed millions of plantation-grown larch in Britain since 2009. To understand the drivers underlying the emergence of *P. pseudosyringae*, we investigated the genetic, morphological, and pathological diversity of *P. pseudosyringae* isolates obtained from various hosts across Britain. Major gene sequence analyses identified two major genetic lineages within the British population of *P. pseudosyringae*. Within these lineages, three host-associated groups (*Fagus–Nothofagus*, *Vaccinium* and *Larix*) could be differentiated based on colony morphology, sporangial size, and in vitro growth characteristics. Moreover, pathogenicity varied markedly between groups with *Larix*-associated isolates producing larger lesions on Japanese larch (*L. kaempferi*) comparable to those formed by *P. ramorum*, whereas *Fagus-Nothofagus-* and *Vaccinium* isolates caused smaller or negligible lesions, respectively. Our findings suggest that *P. pseudosyringae* comprises genetically differentiated lineages that differ in host association, morphology, growth characteristics and pathogenicity. The *Larix*-associated group produced lesions on Japanese larch comparable in size to those caused by *P. ramorum*, suggesting that it has the potential to be an important pathogen of larch in Britain.

Keywords: pathogenicity; clade 3; environmental adaptation; diversity; *Phytophthora ramorum*

Check for updates

Academic Editor: Rimvydas Vasaitis

Received: 24 September 2026
Revised: 3 November 2026
Accepted: 7 November 2026
Published: 11 November 2026

Copyright: © 2026 by the authors. Licensee MDPI, Basel, Switzerland. This article is an open access article distributed under the terms and conditions of the Creative Commons Attribution (CC BY) license.

1. Introduction

Phytophthora pseudosyringae was first formally described in 2003 as a new species within the *P. citricola* complex [1]. The first official report of *P. pseudosyringae* in Britain occurred in 2005, where it was found causing bleeding cankers and lesions on European beech (*Fagus sylvatica*) and hornbeam (*Carpinus betulus*) [2]. However, Brasier and Jung [3] suggested that earlier British records of *P. syringae* on beech, dating back to Day [4], probably referred to *P. pseudosyringae*. The pathogen is now known to occur across Europe [1,5–16], North America [17–19] and Chile [20,21]. In Europe, *P. pseudosyringae* is considered endemic, whereas populations in North America and Chile are thought to be introductions originating from Europe [22]. In Britain, its distribution overlaps with that of the introduced species

P. ramorum and is concentrated in the milder, wetter regions of western Britain (Forest Research, unpublished data).

Prior to 2010, *P. pseudosyringae* was primarily associated with broadleaved hosts in Britain and not regarded as a significant threat to conifer forestry [5,6,14]. It is frequently found affecting the roots and root collars of European beech (*F. sylvatica*) and caused aerial branch and stem cankers on roble beech (*Nothofagus obliqua*), leading to dieback and tree death [14]. It was also linked to less severe infections of raulí beech (*N. procera*) and dieback of bilberry (*Vaccinium myrtillus*) [5,14]. Until recently, detections of *P. pseudosyringae* in British conifer forests were infrequent, but reports have been increasing particularly in association with larch (*Larix* spp.) (unpublished data, Forest Research). Since 2016, multiple larch forests in Britain with symptoms typical of *P. ramorum* infection, such as needle blight, shoot dieback, resinous cankers on the trunk, premature needle loss, and tree mortality, have consistently returned negative results when tested for the presence of *P. ramorum*. Subsequent analysis has often identified *P. pseudosyringae* as the sole agent present in many of these cases. This trend has been particularly evident in Wales, although detections have also been made in England and, less frequently, Scotland (unpublished data, Forest Research). Between 2015 and 2022, the proportion of larch samples from Welsh sites submitted as suspected *P. ramorum* infections that tested positive for *P. pseudosyringae* increased from 9.7% (3/31 samples) to 69.4% (59/85 samples), based on laboratory testing of symptomatic tissues using isolation and molecular methods (unpublished data, Forest Research).

Despite the increasing detections on larch, little is known about the epidemiology of *P. pseudosyringae* in this host. It is typically recovered from necrotic bark lesions on branches but has also occasionally been recovered from foliage, where it is capable of sporulating on larch needles [23]. Historically, *P. pseudosyringae* was not considered a pathogen of conifers, and it was only through *P. ramorum* surveillance activities focused on larch that the first detections were made. However, the consistent detection of *P. pseudosyringae* in symptomatic larch bark in the absence of other pathogens raises the possibility that it may now be causing significant damage to this host.

The lifestyle of *P. pseudosyringae* is variable across hosts and geographic regions. In North America, it is regarded as an aerial pathogen, infecting the foliage and twigs of California bay laurel (*Umbellularia californica*) [18]. In contrast, in continental Europe, it is predominantly soilborne, associated with rhizosphere infections of declining oak, beech, and alder [1]. In Britain, it appears to adopt both lifestyles, sporulating abundantly on the foliage of roble beech and bilberry [14] while also persisting in the rhizosphere of beech, attacking the root collar and extending into the lower stem causing bleeding cankers [2]. This ecological plasticity raises questions about how *P. pseudosyringae* may be interacting with larch and whether a shift in infection strategy could be contributing to its recent emergence on this host.

The emergence of *P. pseudosyringae* on an economically important conifer raises concerns for both commercial forestry and wider environmental health. Initial observations (Forest Research, unpublished observations) suggested that *P. pseudosyringae* caused only localised decline in larch, primarily affecting twigs and small diameter branches, and was not associated with significant tree dieback. However, the role that *P. pseudosyringae* plays in larch dieback has been complicated firstly by the extent of damage caused by *P. ramorum* which has been documented since 2009 [24] and more recently by the detection of both *P. ramorum* and *P. pseudosyringae* DNA in some bark samples (Forest Research, unpublished data), suggesting the potential for concurrent infections. The repeated detection of *P. pseudosyringae* in symptomatic bark samples from declining and dead larch trees suggests that this species may play a more important role in larch decline than was initially recognised.

However, although uncommon, the detection of both *P. pseudosyringae* and *P. ramorum* in some larch samples complicates interpretation of disease outbreaks and raises questions regarding the relative importance of these pathogens in larch decline.

To address some of these uncertainties, in this study, we investigate the genetic, morphological, physiological, and pathological diversity of *P. pseudosyringae* isolates affecting various hosts in Britain with a particular focus on its role in larch dieback. Specifically, we (i) assess the genetic variability of British *P. pseudosyringae* populations; (ii) determine whether genetic differences correspond to phenotypic variation in morphology and growth characteristics; and (iii) evaluate the pathogenic potential of *P. pseudosyringae* in larch bark relative to *P. ramorum*, assessing its capacity to act as a significant pathogen.

2. Materials and Methods

2.1. Isolates and Growth on Agar Media

A total of 51 isolates of *P. pseudosyringae* (Table 1) were obtained from the Forest Research culture collection. The isolates originated from infected host plants and trees sampled during diagnostic surveys and field investigations in forest settings across the British Isles between 2009 and 2018. Species identity was confirmed through the sequence analyses described below. All isolates were purified by single hyphal-tip isolation prior to subsequent analyses and maintained on carrot agar (CA) prepared as described by Brasier and Kirk [25], incubated at 20 °C in darkness for the duration of the experimental work. To obtain enough mycelium for genetic studies, isolates were grown on CA plates, where the agar surface was covered with a disc of sterilised cellophane and incubated at 20 °C for two weeks. Mycelium was then scraped from the cellophane, with ca. 50 mg placed in a microtube and stored at −80 °C until required.

Table 1. Details of phytophthora isolates used in the study.

Isolate	Species	Sampled Host	Host Material	Year	Location	Experiment *
P2173	*P. pseudosyringae*	*Nothofagus procera*	unknown	2009	Cornwall, England	M
P2491	*P. pseudosyringae*	*Fagus sylvatica*	Bark	2011	Hampshire, England	M
P2493	*P. pseudosyringae*	*Nothofagus obliqua*	Bark	2011	Hampshire, England	M
P2494	*P. pseudosyringae*	*Nothofagus obliqua*	Bark	2011	Hampshire, England	M, G, S, P
P2495	*P. pseudosyringae*	*Nothofagus obliqua*	Shoots	2011	Hampshire, England	M
P2496	*P. pseudosyringae*	*Nothofagus obliqua*	Bark	2011	Hampshire, England	M
P2497	*P. pseudosyringae*	*Nothofagus obliqua*	Foliage	2011	Hampshire, England	M
P2503	*P. pseudosyringae*	*Vaccinium myrtillus*	Foliage	2011	Dartmoor, England	M
P2506	*P. pseudosyringae*	*Nothofagus procera*	Foliage	2011	Argyll and Bute, Scotland	M
P2507	*P. pseudosyringae*	*Nothofagus procera*	Bark	2011	Argyll and Bute, Scotland	M
P2509	*P. pseudosyringae*	*Nothofagus procera*	Bark	2011	Argyll and Bute, Scotland	M
P2514	*P. pseudosyringae*	*Nothofagus procera*	Foliage	2011	Cumbria, England	M
P2515	*P. pseudosyringae*	*Nothofagus procera*	Foliage	2011	Cumbria, England	M
P2543	*P. pseudosyringae*	*Nothofagus obliqua*	Bark	2011	Conway, Wales	M
P2731	*P. pseudosyringae*	unknown	Bark	2011	Somerset, England	M
P2831	*P. pseudosyringae*	*Vaccinium myrtillus*	Foliage	2013	Cumbria, England	M, G, S, P
P2837	*P. pseudosyringae*	*Vaccinium myrtillus*	Foliage	2013	England	M
P2841	*P. pseudosyringae*	*Fagus sylvatica*	Bark	2013	Monmouthshire, Wales	M
P2842	*P. pseudosyringae*	*Vaccinium myrtillus*	Foliage	2013	Denbighshire, Wales	M, G, S, P
P2871	*P. pseudosyringae*	*Nothofagus*	Bark	2013	Gwynedd, Wales	M
P2872	*P. pseudosyringae*	*Nothofagus*	Bark	2013	Gwynedd, Wales	M
P2928	*P. pseudosyringae*	*Fagus sylvatica*	Bark	2014	Somerset, England	M, G, S, P
P2929	*P. pseudosyringae*	*Fagus sylvatica*	Bark	2014	Somerset, England	M
P2941	*P. pseudosyringae*	unknown	unknown	unknown	unknown	M
P2951	*P. pseudosyringae*	unknown	Bark	2015	unknown	M
P2965	*P. pseudosyringae*	*Nothofagus obliqua*	Bark	2014	Argyll and Bute, Scotland	M
P3007	*P. pseudosyringae*	*Fagus sylvatica*	Bark	2015	England	M
P3005	*P. pseudosyringae*	*Nothofagus*	Bark	2015	Somerset, England	M
P3006	*P. pseudosyringae*	*Fagus sylvatica*	Bark	2015	England	M
P3008	*P. pseudosyringae*	*Nothofagus*	Foliage	2014	Devon, England	M
P3029	*P. pseudosyringae*	*Fagus sylvatica*	Bark	2015	Cardiff, Wales	M, G, S, P

Table 1. *Cont.*

Isolate	Species	Sampled Host	Host Material	Year	Location	Experiment *
P3034	*P. pseudosyringae*	*Fagus sylvatica*	Bark	2015	Cardiff, Wales	M
P3043	*P. pseudosyringae*	*Larix*	Bark	2015	Northern Ireland	M
P3086	*P. pseudosyringae*	*Vaccinium myrtillus*	Foliage	2015	Staffordshire, England	M
P3090	*P. pseudosyringae*	*Vaccinium myrtillus*	Foliage	2015	Staffordshire, England	M, G, S, P
P3092	*P. pseudosyringae*	*Vaccinium myrtillus*	Foliage	2015	Staffordshire, England	M
P3093	*P. pseudosyringae*	*Vaccinium myrtillus*	Foliage	2015	Staffordshire, England	M
P3097	*P. pseudosyringae*	*Nothofagus*	Foliage	2015	Argyll and Bute, Scotland	M
P3108	*P. pseudosyringae*	*Fagus sylvatica*	Bark	2015	Cumbria, England	M
P3193	*P. pseudosyringae*	*Fagus sylvatica*	Bark	2015	Gloucestershire, England	M
P3200	*P. pseudosyringae*	*Tilia*	Bark	2015	Yorkshire, England	M
P3205	*P. pseudosyringae*	*Fagus sylvatica*	Bark	2015	Gloucestershire, England	M
P3245	*P. pseudosyringae*	*Vaccinium myrtillus*	Foliage	2015	Staffordshire, England	M
P3252	*P. pseudosyringae*	*Nothofagus*	Bark	2015	Gloucestershire, England	M
P3549	*P. pseudosyringae*	*Nothofagus procera*	unknown	2018	Pembrokeshire, Wales	M, G, S, P
P3550	*P. pseudosyringae*	*Vaccinium myrtillus*	Foliage	2018	unknown	M, G, S, P
P3551	*P. pseudosyringae*	*Larix kaempferi*	Bark	2017	Powys, Wales	M, G, S, P
P3552	*P. pseudosyringae*	*Larix kaempferi*	Bark	2017	Powys, Wales	M, G, S, P
P3553	*P. pseudosyringae*	*Larix*	Bark	2017	Powys, Wales	M, G, S, P
P3554	*P. pseudosyringae*	*Larix*	Bark	2017	Powys, Wales	M
P3555	*P. pseudosyringae*	*Larix*	Bark	2018	Powys, Wales	M, G, S, P
P3048	*P. ramorum:* EU1	*Larix kaempferi*	Bark	2010	Somerset, England	P
P3900	*P. pluvialis*	*Tsuga heterophylla*	Bark	2021	Cornwall, England	M
TJ0041	*P. ilicis*	*Ilex aquilifolium*	unknown	unknown	UK	M
TJ0319	*P. psychrophila*	*Quercus ilex*	unknown	unknown	La Mancha, Spain	M
TJ1169	*P. nemorosa*	*Viburnum davidii*	Foliage	2017	Croatia	M

* M—multigene analysis, G—growth rate, S—sporangia size, P—pathogenicity.

2.2. Genetic Analysis—Multi-Locus Sequencing and Phylogenetic Analysis

Analysis was performed on all 51 isolates of *P. pseudosyringae* (50 from British woodlands and one from Northern Ireland). Sequencing was also performed on one isolate of each species of *Phytophthora* from ITS clade 3; *P. ilicis*, *P. nemorosa*, *P. pluvialis* and *P. psychrophila* (Table 1).

2.2.1. DNA Extraction, Amplification and Sequencing

Genomic DNA was extracted from mycelium using KingFisherTM Plant DNA kits (Thermo Scientific™ Waltham, MA, USA) on a KingFisher™ Flex Magnetic Particle Processor (Thermo Scientific™ Waltham, MA, USA), following the manufacturer's instructions. Phytophthora isolates were sequenced at six gene regions (Table 2). Loci were amplified using a PCR mixture of 10–20 ng of template DNA. Each reaction contained 1× (i.e., 12.5 µL) GoTaq Green Master Mix (Promega, Madison, WI, USA) and 0.4 µM of each primer in a total volume of 25 µL. Amplifications were performed with an Applied Biosystems Proflex PCR thermal cycler (Thermo Fisher Scientific corporation, Foster City, CA, USA) using the following cycling protocol: denaturation step of 94 °C for 2 min; 35 cycles of 94 °C for 30 s, the locus-specific annealing temperature for 30 s, with a 72 °C extension for 60 s; and final extension of 5 min at 72 °C. Successful amplification was confirmed by gel electrophoresis. PCR products were prepared for sequencing using DNA Clean & Concentrator-5 (Zymo Research, Irvine, CA, USA) as per manufacturer's instructions and sequenced in both forward and reverse directions by Source BioScience Limited (Nottingham, UK). Chromatograms were visually inspected using Sequencher (version 5.4.6), and any ambiguous base calls were resolved by comparison of forward and reverse reads prior to generation of consensus sequences. Consensus sequences were subsequently used for downstream analyses.

Table 2. Primers used in this study.

Locus	Genome	Primer	Primer Sequence (5′-3′)	T *	Reference
Beta-tubulin (B-tub)	Nuclear	Btub_F1 Btub_R1	GCCAAGTTCTGGGAGGTCATC CCTGGTACTGCTGGTACTCAG	60	[26]
NADH Dehydrogenase subunit 1 (NADH)	Mitochondrial	NADH_F1 NADH_R1	CTGTGGCTTATTTTACTTTAG CAGCAGTATACAAAAACCAAC	53	[27]
Elongation factor 1 Alpha (EF)	Nuclear	EF1A_for EF1A_rev	TCACGATCGACATTGCCCTG ACGGCTCGAGGATGACCATG	60	[27]
Internal transcribed spacer region (ITS)	Nuclear	ITS4 ITS6	TCCTCCGCTTATTGATATG GAAGGTGAAGTCGTAACAAGG	55	[28]
Cytochrome c oxidase I (COX1)	Mitochondrial	Oom COX1-levup FM 85 mod	TCAWCWMGATGGCTTTTTTCAAC RRHWACKTGACTDATRATAC-CAAA	54	[29]
Cytochrome c oxidase II (COX2)	Mitochondrial	Cox2F Cox2-RC4	GGCAAATGGGTTTTCAAGATCC TGATTWAYNCCACAATTTCRCTA-CATTG	54	[30]

* T—Annealing temperature (°C).

2.2.2. Phylogenetic Analyses

Phylogenetic analyses were conducted using both maximum likelihood and Bayesian approaches. Sequences were aligned with MUSCLE in Geneious Prime 2022.0.2 software. For the maximum likelihood approach, PartitionFinder 2 [31] was first used to find the best-fit partitioning schemes and evolutionary models based on the corrected Akaike Information Criterion (AICc) using linked branch lengths. The largest set of possible models was investigated (the option models = allx;), and all possible partitioning schemes were tested (option search = all;). RAxML-NG v1.1.0 [32] was used to construct the phylogenies. The adequate number of bootstraps was determined using the MRE-based bootstopping test [33], with a maximum of 20,000 replicates. Bayesian inference analyses were performed using BEAST 2 [34]. The uncorrelated lognormal relaxed molecular clock model [35] was used in all cases. Two independent runs were conducted, each with a chain length of 40 million generations. Posterior estimates of the parameters were summarised with Tracer [36] and their quality assessed by a visual appraisal of the trace plots and ESS values. Trace and tree samples were combined using LogCombiner 2.6.1 (part of BEAST 2), and subsequently, TreeAnotator (part of BEAST 2) was used to create maximum clade credibility trees using a burn-in of 10%.

Phylogenetic trees were visualised in TreeGraph2 v. 2.15.0-887 beta [37]. Support values from the maximum-clade-credibility Bayesian inference trees were mapped onto the best-scoring maximum likelihood trees, and branch lengths were displayed as branch thickness to aid visualization of numerous long branches. Phylogenetic analyses were initially conducted separately for each gene region. As the resulting trees were highly similar, two concatenated analyses were conducted, one for all nuclear genes and another for all mitochondrial genes.

2.3. Morphological and Physiological Assessment

Twelve isolates of *P. pseudosyringae* identified in the genetic analysis as belonging to three host-associated groups (Table 1, isolates denoted by the letters G, S, and P in the Experiment column) were used to test for the presence of morphological and/or physiological differences. Four isolates were selected from each host-associated group to provide replication across groups while maintaining a practical number of isolates for detailed morphological, physiological, and pathogenicity assessments. The selected isolates comprised

representative members of the three host-associated groups identified by the phylogenetic analyses. Morphological differences were assessed by examining colony type and measuring the length and breadth of sporangia. Physiological properties of the same isolates were examined through in vitro growth temperature responses. All isolates were passaged once through detached foliage of their original host prior to experimentation to minimise any reduction in pathogenicity associated with prolonged maintenance in culture. Following lesion development, isolates were re-isolated onto selective medium (SMA) and subcultured prior to use in experiments. All isolates underwent the same passage procedure prior to experimentation.

2.3.1. Morphology

Colony morphology was assessed by growing isolates on CA in the dark for 10 days at 20 °C. Four plates were used for each isolate, with each colony pattern type being categorised. Sporangia sizes were assessed by growing isolates on CA incubated in the dark for 7 days at 20 °C. Ten disks, each 15 mm in diameter, were then cut from the growing edge of the 7d old cultures and placed in a Petri dish (one dish per isolate). The plates were flooded with sterile filtered pond water and incubated for 10 days in natural light at 20 °C. One hundred randomly chosen mature sporangia from each isolate were observed on the disks under a microscope at x 400 magnification and length and breadth measurements recorded. A length x breadth ratio (l/b ratio) was then generated for each sporangium.

Morphological data were analysed in R version 3.5.2 [38]. Differences in sporangial l/b ratio among genetic groups were analysed using a linear mixed-effects model fitted with the lme4 package [39]. The l/b ratio was treated as the response variable, genetic group as a fixed effect, and isolate as a random effect to account for repeated measurements within isolates. The response variable was log-transformed to improve model fit and reduce residual heterogeneity. Estimated marginal means were calculated using the emmeans package [40], and Tukey-adjusted pairwise comparisons were used to assess differences among genetic groups.

2.3.2. Physiology—In Vitro Growth Temperature Response

The growth rates of the same 12 isolates were measured on three different media: carrot agar (CA), V8 agar, and potato dextrose agar (PDA), prepared according to published methods [25,41,42], respectively. The three agar types were selected to put isolates under an array of environmental stresses, thereby revealing any differences amongst them. CA and V8 agar were used as they are typically used for culturing phytophthoras, with V8 agar considered to provide slightly more nutrient stress than CA [41]. PDA provided the most 'stressful' environment due to its high sugar concentration and lack of plant sterols which are required by phytophthoras for growth stimulation and sporulation [43]. Plates were inoculated centrally and incubated in the dark at six temperatures: 5, 10, 15, 20, 25, 30 °C. Four radial growth measurements were made on each colony to generate an average as described previously [44]. Four plates were used for each isolate/agar/temperature combination, and the entire experiment was performed twice (trial 1 and trial 2) using the same isolates.

In vitro growth temperature response data were analysed in R version 3.5.2 [38]. Differences in growth rate among host-associated groups were analysed using linear mixed-effects models. Linear growth rate was treated as the response variable, isolate group as a fixed effect, and temperature and isolate as random effects. Estimated marginal means were calculated to compare growth rates among host-associated groups, and Tukey-adjusted pairwise comparisons were used to identify significant differences. Growth rates differed among agar media; therefore, each medium was analysed separately. A trial effect was

also observed, with overall growth rates differing between trial 1 and trial 2 despite the use of the same isolates, media, and incubation conditions. Consequently, the two trials were analysed independently using the same modelling approach, rather than pooled into a single analysis.

2.4. Assessment of Pathogenic Potential on Larch Bark

A laboratory-based experiment was conducted to investigate the pathogenicity of *P. pseudosyringae* using *P. ramorum* as a benchmark pathogen for comparison on larch bark. The inner bark (phloem) of Japanese larch (*L. kaempferi*) was challenged with mycelial plugs of the twelve isolates of *P. pseudosyringae* and one isolate of *P. ramorum* (Table 1). The EU1 lineage was selected as it represents the predominant *P. ramorum* clonal lineage affecting larch in Britain.

The methodology followed a previously published protocol [45]. Potted larch saplings from the Forest Research intensive nursery were selected for the experiment. Saplings were approximately 1.5 m in height and 1.5–2.0 cm in stem diameter. Five equidistant inoculation points were positioned at least 10 cm from both the base and the top of the stem over the stem length. Inoculation involved making a wound by removing a 2.5 mm bark disc using a sterilized cork borer, followed by the insertion of a 2.5 mm CA plug taken from the margin of a Phytophthora colony. Cotton wool soaked in sterile distilled water (SDW) was applied to the inoculation point and secured in place with a strip of Parafilm. Inoculated trees were incubated in a growth chamber at 20 °C under 12 h light/ 12 h dark regime for 8 weeks. On each stem, five wounds were inoculated: three isolates of *P. pseudosyringae* (one representing each host-associated genetic group), one isolate of *P. ramorum* (EU1 lineage), and a control consisting of a sterile CA plug. Each isolate was randomly allocated to an inoculation position on the stem.

In total, 20 saplings were inoculated, generating 5 replicates of each of the 12 isolates of *P. pseudosyringae* and 20 replicates of *P. ramorum* and the control. Following incubation, necrotic tissue areas surrounding each inoculation point were quantified. The phloem tissue was exposed with a scalpel, and the lesion boundaries outlined on Parafilm® wrapped around the stem at the exposed lesion site. The traced lesion areas were subsequently calculated using ImageJ v1.54k (National Institutes of Health, Bethesda, MD, USA) software [46]. To confirm that any necrosis was due to the agent inoculated, isolations were made from the necrotic phloem tissue at the end of each lesion by removing and aseptically plating tissue chips onto Phytophthora selective medium (a modification of synthetic mucor agar) as described previously [47]. Identity of any outgrowths was based on spore structures. The experiment was conducted twice, once in autumn 2022 (autumn trial), and once in late spring of 2023 (spring trial).

Pathogenicity data were analysed using R version 4.4.2 [48]. Differences in pathogenicity among the three host-associated groups of *P. pseudosyringae* and *P. ramorum* were analysed using general linear mixed models (GLMMs). Pathogenicity was measured as lesion area (cm^2) and was log-transformed to improve model fit. Pathogen was included as a categorical fixed effect (*P. pseudosyringae Fagus-Nothofagus*, *Larix*, *Vaccinium*, *P. ramorum*, and a control). Data from all isolates within each *P. pseudosyringae* group were pooled for analysis. Inoculation position was included as an additional numeric fixed effect, as lesion area was generally observed to decrease from the top to the bottom of the tree. All models included a random effect of tree. Models were fitted using maximum likelihood in lme4 [39] with lmerTest [49]. The significance of fixed effects was assessed using *F*-tests implemented in the drop1 function, with degrees of freedom estimated using the Satterthwaite approximation. Pairwise comparisons among treatments were conducted using Tukey-adjusted contrasts in emmeans [40].

3. Results

3.1. Multi-Locus Sequencing and Phylogenetic Analyses

Sequencing of six loci (three nuclear and three mitochondrial) was carried out on 51 isolates of *P. pseudosyringae* and 1 isolate of each from the 4 other species within ITS clade 3; *P. ilicis*, *P. nemorosa*, *P. pluvialis* and *P. psychrophila*. For each isolate, consensus sequences were generated for each locus from forward and reverse Sanger sequencing reads. All sequences generated in this study have been deposited in GenBank. Accession numbers for each isolate and locus are provided in Supplementary Table S1. In total, the concatenated nuclear dataset comprised 2509 bp (*B*-tub 900 bp; EF 842 bp; ITS 767 bp), whilst the concatenated mitochondrial dataset comprised 2045 bp (Cox1 685 bp; Cox2 585 bp; NADH 775 bp). Maximum likelihood and Bayesian inference analyses produced identical topologies for both datasets.

Both the nuclear and mitochondrial gene trees (Figures 1 and 2, respectively) produced two highly supported lineages (with bootstrapping values of 80 and 98% respectively). One lineage comprised isolates primarily from *Fagus* and *Nothofagus*, while the other was composed almost entirely of isolates from *Vaccinium* and *Larix*. In the mitochondrial tree (Figure 2), the *Vaccinium-Larix*-associated group split further into host-specific clusters (bootstrap 79%), a pattern mirrored in the nuclear tree (bootstrap 74%), although two *Vaccinium* isolates grouped with the *Larix* cluster in the nuclear gene tree. In contrast, the mitochondrial tree of the *Fagus-Nothofagus* lineage showed only moderate support for further subdivision (bootstrap 63%), but with no corresponding split in the nuclear tree.

3.2. Morphological and Behavioural Assessment

3.2.1. Colony Patterns

Isolates of *P. pseudosyringae* generated three distinct colony patterns when grown on CA, corresponding to host association: *Vaccinium*-associated isolates produced stellate patterns, *Larix*-associated isolates formed radiate patterns, and *Fagus-Nothofagus* isolates exhibited rosaceous patterns (Figure 3).

3.2.2. Sporangia Size

All isolates produced sporangia, with variation in abundance and size (Table 3). On average, the *Larix* associated isolates had the longest sporangia (51.2 ± 0.9 µm), followed by *Vaccinium* (46.5 ± 0.8 µm), while *Fagus-Nothofagus* were shortest (43.8 ± 0.9 µm). Sporangial widths were similar across groups (Table 3). The largest average l/b ratio was recorded in isolate P3552 (*Larix* associated isolate) at 1.83 ± 0.02, while the smallest was in P2928 (*Fagus-Nothofagus* associated isolate at 1.33 ± 0.01). When data were pooled by genetic group, mean sporangia l/b ratios differed significantly ($p = 0.013$). The *Larix* associated isolates had significantly higher l/b ratios than both the *Vaccinium* associated isolates ($\beta = -0.13$, SE = 0.04, $p = 0.03$) and the *Fagus-Nothofagus* isolate group ($\beta = -0.16$, SE = 0.00, $p = 0.006$). There was no statistically significant difference between *Vaccinium* and *Fagus-Nothofagus* host-associated groups ($\beta = -0.03$, SE = 0.04, $p = 0.76$) (Figure 4).

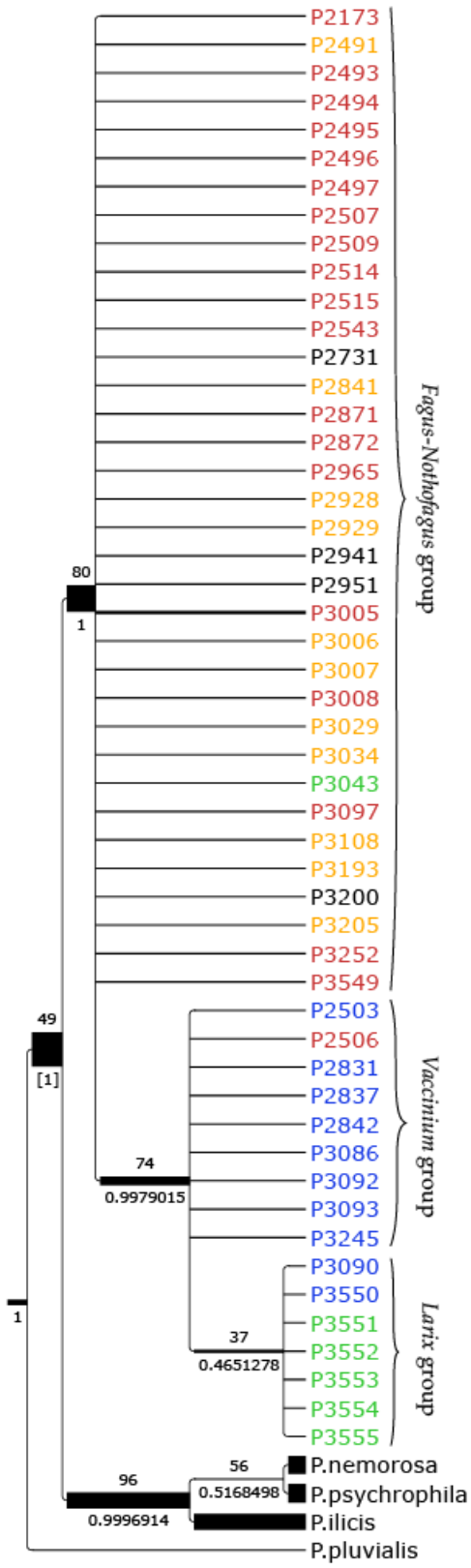


Figure 1. Maximum likelihood tree of *P. pseudosyringae* based on concatenated nuclear genes. Branch thickness represents the length of the branch. Bootstrap values (from the ML tree) are displayed above the branch, and posterior probabilities (from the Bayesian tree) are displayed below the branch. To simplify tree visualization, ML and Bayesian nodes with bootstrap support < 30% and posterior probability < 0.2, respectively, were collapsed. Colours denote the host association; yellow = *Fagus*, red = *Nothofagus*, blue = *Vaccinium*, green = *Larix*, black = unknown.

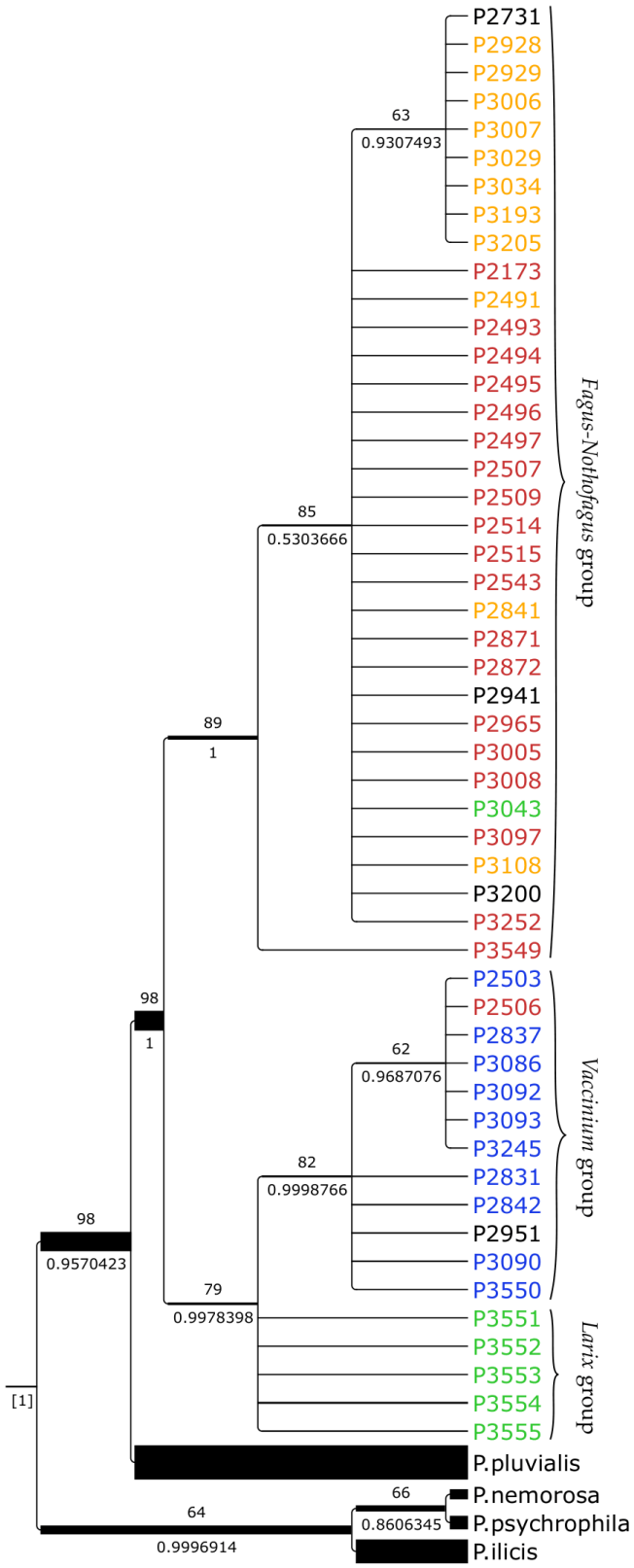


Figure 2. Maximum likelihood tree of *P. pseudosyringae* based on concatenated mitochondrial genes. Branch thickness represents the length of the branch. Bootstrap values (from the ML tree) are displayed above the branch, and posterior probabilities (from the Bayesian tree) are displayed below the branch. To simplify tree visualization, ML and Bayesian nodes with bootstrap support < 60% and posterior probability < 0.5, respectively, were collapsed. Colours denote the host association; yellow = *Fagus*, red = *Nothofagus*, blue = *Vaccinium*, green = *Larix*, black = unknown.

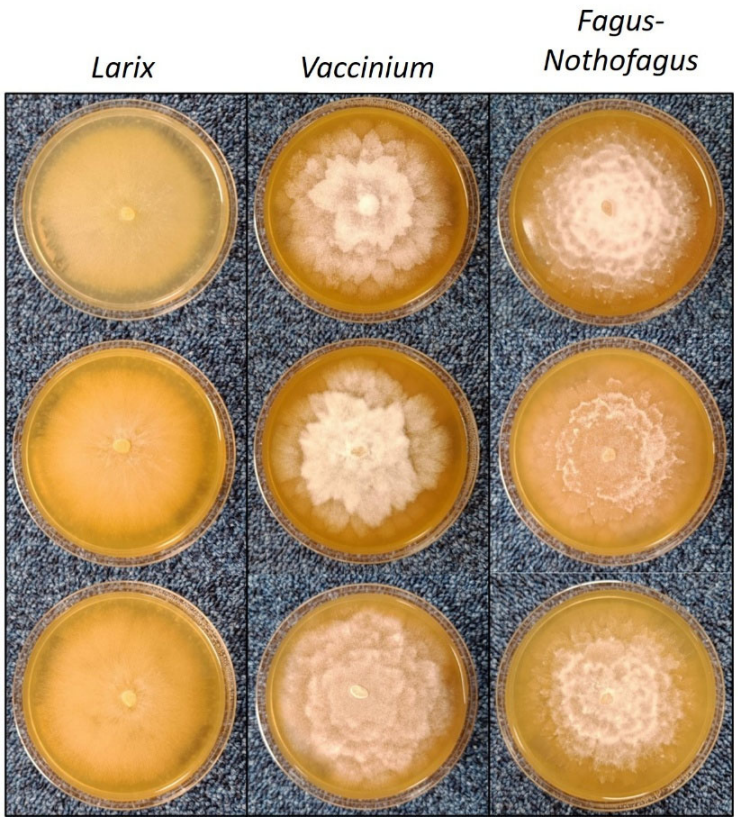


Figure 3. Variability of colony types among representative *P. pseudosyringae* isolates from the three host-associated groups identified in the phylogenetic analyses. *Larix*-associated isolates show radiate patterns, *Vaccinium*-associated isolates show stellate patterns, and *Fagus–Nothofagus*-associated isolates show rosaceous patterns.

Table 3. Sporangia characteristics of representative *Phytophthora pseudosyringae* isolates from the three host-associated groups identified in the phylogenetic analyses, grown on carrot agar (CA) at 20 °C. A total of 100 sporangia were measured for each isolate.

Host-Associated Group *	Isolate	Length Range (µm)	Breadth Range (µm)	Mean Length × Breadth (µm (±1 s.e.))	l/b Ratio (±1 s.e)
Vaccinium	P2842	78.09–29.81	43.07–21.26	51 (±0.9) × 33 (±0.5)	1.54 (±0.02)
	P3090	70.09–31.37	43.38–18.69	51 (±0.8) × 34 (±0.5)	1.51 (±0.02)
	P3550	51.44–25.47	36.4–18.92	39 (±0.4) × 29 (±0.4)	1.34 (±0.01)
	P2831	61.39–31.34	47.42–23.56	45 (±0.6) × 32 (±0.3)	1.44 (±0.02)
Larix	P3553	64.49–29.21	38.86–20.52	47 (±0.7) × 30 (±0.4)	1.56 (±0.01)
	P3551	75.35–27.92	46.28–20.27	54 (±0.9) × 33 (±0.5)	1.64 (±0.02)
	P3552	81.49–30.29	38.05–18.44	54 (±1.0) × 29 (±0.4)	1.83 (±0.02)
	P3555	73.66–26.11	44.73–19.37	51 (± 0.7) × 31 (±0.3)	1.62 (±0.02)
Fagus-Nothofagus	P3549	71.74–34.15	51.74–27.32	52 (±0.7) × 38 (±0.4)	1.39 (±0.01)
	P2494	62.66–28.25	44.43–19.59	44 (±0.7) × 32 (±0.4)	1.35 (±0.01)
	P2928	58.83–25.53	34.67–20.69	38 (±0.7) × 28 (±0.3)	1.33 (±0.01)
	P3029	69.43–26.26	39.26–18.04	42 (±0.9) × 28 (±0.4)	1.47 (±0.02)

* The host-associated group refers to the *Vaccinium*, *Larix*, and *Fagus-Nothofagus* groups delineated by the phylogenetic analysis. See main text for details.

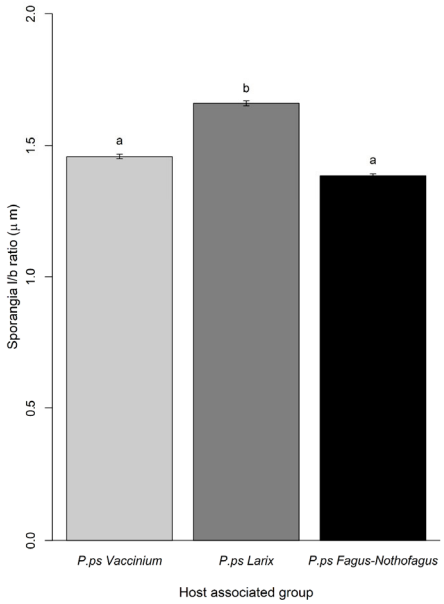


Figure 4. Mean sporangia length/breadth (l/b) ratio of representative *Phytophthora pseudosyringae* isolates from the three host-associated groups identified in the phylogenetic analyses. Lettering above the bars indicates significant differences among host-associated groups (groups not sharing a letter are significantly different at $p < 0.05$).

3.2.3. In Vitro Growth Temperature Response

Growth rates were measured across six temperatures (5–30 °C) on CA, V8, and PDA media. On CA, all host-associated groups displayed similar growth curves, with optimum growth at 20 °C. *Larix* isolates grew at 25 °C, unlike *Vaccinium* and *Fagus-Nothofagus* groups, which did not grow at 25 °C. No growth occurred at 30 °C for any isolate, but all host-associated groups showed detectable growth at 5 °C. Mean growth rates differed significantly (Table 4). *Larix*-associated isolates grew significantly faster than both *Vaccinium* and *Fagus-Nothofagus*-associated isolates. The *Fagus-Nothofagus* isolate group had slightly higher growth rates than *Vaccinium*, but this was statistically significant only in the second trial. On V8 agar, similar temperature patterns were observed. However, *Fagus-Nothofagus*-associated isolates were fastest growing, followed by *Larix*, with *Vaccinium* the slowest, but the differences were not statistically supported. On PDA, growth was markedly slower across all groups, with an optimum at 15 °C. No growth was recorded at 25 °C or 30 °C. *Larix* isolates grew significantly faster than *Fagus-Nothofagus*, which in turn grew faster than *Vaccinium* isolates (Figure 5).

Table 4. Statistical contrast groupings of the mean growth rates of the three host-associated groups (*Vaccinium*, *Larix* and *Fagus-Nothofagus*) of *Phytophthora pseudosyringae* isolates over the temperature range 5–25 °C.

		***p* Value**		**Contrast Grouping**		
		Trial			**Trial**	
Agar	**Contrasts**	**1**	**2**	**Isolate Group**	**1**	**2**
CA †	*Vaccinium*/*Larix*	**0.04**	**0.03**	*Vaccinium*	a	a
	Vaccinium/*Fagus-Nothofagus*	0.42	0.99	*Larix*	b	b
	Larix/*Fagus-Nothofagus*	0.34	**0.02**	*Fagus-Nothofagus*	a	c
V8 †	*Vaccinium*/*Larix*	0.37	0.13	*Vaccinium*	a	a
	Vaccinium/*Fagus-Nothofagus*	0.85	0.63	*Larix*	a	a
	Larix/*Fagus-Nothofagus*	0.67	0.46	*Fagus-Nothofagus*	a	a

Table 4. *Cont.*

		p Value		Contrast Grouping		
		Trial			Trial	
Agar	**Contrasts**	**1**	**2**	**Isolate Group**	**1**	**2**
PDA †	*Vaccinium*/*Larix*	**0.00**	**0.00**	*Vaccinium*	a	a
	Vaccinium/*Fagus-Nothofagus*	0.16	0.39	*Larix*	b	b
	Larix/*Fagus-Nothofagus*	**0.00**	**0.00**	*Fagus-Nothofagus*	a	a

† CA = carrot agar; V8 = V8 vegetable juice agar; PDA = potato dextrose agar. Trials refers to the two independent growth rate experiments. Different letters indicate statistically significant differences between isolate groups within a trial and agar medium ($p < 0.05$); groups sharing the same letter are not significantly different.

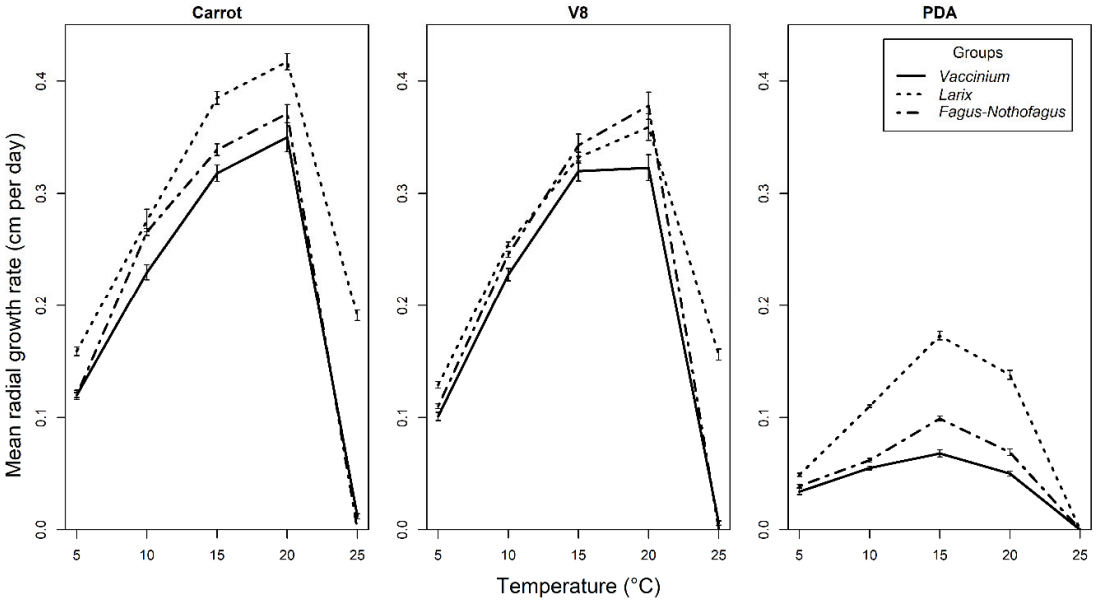


Figure 5. Mean radial growth rates of *Phytophthora pseudosyringae* isolates from the three host-associated groups (*Vaccinium*, *Larix* and *Fagus-Nothofagus*) over the temperature range 5 °C to 30 °C on carrot agar (CA), V8 agar (V8) and potato dextrose agar (PDA).

3.2.4. Pathogenic Potential on Larch Bark

All isolates of *P. pseudosyringae* caused necrosis in the phloem of Japanese larch saplings in both seasonal experiments (the autumn trial and late spring trial); there was little or no necrosis in the controls. The inoculated pathogen was successfully reisolated from all lesions assessed, confirming that lesion development was associated with the inoculated isolates. Lesion size varied significantly by season, with larger lesions occurring in autumn compared to late spring, so data from the two experiments (autumn trial and spring trial) were analysed separately. In both trials, host association had a significant effect on lesion area (Autumn 2022: F 4,80 = 28.31, $p < 0.001$; Spring 2023: F 4,99 = 22.50, $p < 0.001$). In late spring, lesions produced by *Larix*-associated isolates did not differ significantly from those caused by *P. ramorum*. In contrast, *Vaccinium* and *Fagus-Nothofagus* associated isolates produced significantly smaller lesions, indistinguishable from controls (Figure 6b). In autumn, lesions tended to be larger compared to the spring. However, the lesions formed by both *Larix* and *Fagus-Nothofagus* isolates did not differ significantly from those caused by *P. ramorum*, while *Vaccinium* isolates again induced minor lesions that did not differ significantly from the controls (Figure 6a). In both trials, inoculation position influenced lesion size, with a general decrease from top to bottom of the tree. This trend was marginally non-significant in spring (F 1,80 = 3.16, $p = 0.08$) but significant in autumn (F 1,99 = 8.46, $p = 0.005$).

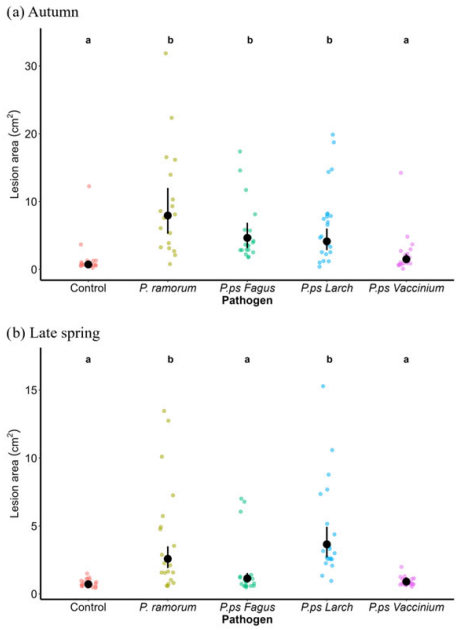


Figure 6. Comparative pathogenicity of the three host-associated groups of *P. pseudosyringae* and *P. ramorum* EU1 on Japanese larch (*Larix kaempferi*) based on lesion size following inoculation of bark tissue in (**a**) autumn and (**b**) late spring. Colours of raw data points correspond to pathogen type, and black points with error bars denote estimated marginal means and 95% confidence intervals for each pathogen. Estimated marginal means and confidence intervals are back-transformed from the log scale and averaged over the effect of inoculation position on the tree. Letters denote statistically significant differences between groups ($p < 0.05$), where pathogens that share a common letter do not show a statistically significant difference in lesion area.

4. Discussion

This study provides new insights into the diversity and potential ecological differentiation within *P. pseudosyringae* populations in Britain, highlighting a possible emerging role in causing dieback of larch. Regarded in Europe as a broadleaf, root and rhizosphere-associated pathogen, our findings reveal that in Britain *P. pseudosyringae* comprises at least two genetically differentiated lineages with differing host associations and pathogenic potential. These results are consistent with earlier reports of host-linked variation in morphology and pathogenicity and support previous suggestions that divergence may still be occurring within *P. pseudosyringae* and that the species comprises multiple genetically differentiated lineages [1,7,22].

Molecular analyses identified two major lineages within the British population: one primarily associated with *Fagus-Nothofagus* and another with *Vaccinium* and *Larix*. These lineages correspond to those previously identified in the global population study of [22], who used genotyping-by-sequencing (GBS) to investigate population structure and outcrossing in the species. Specifically, the *Fagus-Nothofagus* and *Larix-Vaccinium* lineages correspond to the DAPC5 and DAPC1 lineages, respectively, described by [22]. Importantly, the present study demonstrates that the major lineages previously identified using genotyping-by-sequencing [22] can also be distinguished using conventional Sanger sequencing of selected loci, providing a more accessible approach for routine lineage identification.

While *P. pseudosyringae* is already known to be genetically diverse [18,22,50], our findings strongly suggest this diversity is functionally significant. Differences in colony morphology, sporangial size, and growth rates among the three host-associated groups demonstrate that genetic differentiation within *P. pseudosyringae* is associated with pheno-

typic variation. These findings are consistent with host-associated differentiation, although the extent of host specialisation and adaptive divergence remains to be established. Although isolates were sampled from multiple regions of Britain, the host-associated groups were not evenly distributed geographically. Consequently, it was difficult to distinguish the effects of host association from those of geographic origin, and some of the observed genetic and phenotypic differentiation may reflect geographic structure, environmental variation, host association, or a combination of these factors. The *Larix* group, for example, consistently produced larger sporangia, was faster growing, and had a higher maximum growth temperature. These traits could potentially provide adaptive advantages in canopy microclimates, where elevated temperatures and larger sporangia could enhance aerial dispersal. In contrast, the characteristics of *Vaccinium* isolates may be consistent with local dispersal and persistence near the forest floor. These ecological differences, while not definitive, suggest that group-specific phenotypic traits could reflect different dispersal strategies or habitat preferences. This interpretation is consistent with observations [22], which showed that isolates belonging to DAPC1 (i.e., the *Vaccinium* group of this study) were more frequently recovered from rivers and streams than those in DAPC5 (i.e., the *Fagus-Nothofagus* group of this study), suggesting differences in habitat association or dispersal ecology between genetic groups. Variation in sporangial caducity among isolates of *P. pseudosyringae* has previously been reported [1], which may support this hypothesis, as caducity is closely linked to dispersal mechanisms. Although caducity was not assessed in the present study, future investigation of this and other reproductive traits may help determine whether ecological niche differentiation is occurring among genetically differentiated groups. Interestingly, while the *Larix* and *Vaccinium* groups clustered together within the same major lineage in both the nuclear and mitochondrial phylogenies, they consistently differed in phenotype across all experiments. The *Fagus–Nothofagus* isolates showed more variable relationships with the other two groups depending on the trait assessed. This pattern of overlapping yet distinct traits may suggest past hybridisation or gene flow between groups, particularly in environments where multiple hosts coexist. Hybridisation has been observed in other Phytophthora species complexes (e.g., *P. alni*, *P.* × *cambivora* [51]) and may similarly be contributing to the evolution of *P. pseudosyringae*. Evidence of admixture and outcrossing within the global population of this species [22] lends support to this hypothesis. Alternatively, these patterns could also result from convergent adaptation to similar ecological niches, or from habitat filtering where isolates with particular traits are more likely to persist under specific environmental conditions.

Phytophthora pseudosyringae is known to exhibit ecological and lifestyle variability across its range, typically being an aerial pathogen in North America but associated with the rhizosphere in Europe. Within Britain, it occupies both ecological niches, as an aerial pathogen on *N. obliqua* [14] but a soil and root dwelling pathogen on *Fagus* and *Carpinus* [2]. The occurrence of a *Larix*-associated group that appears to occupy an aerial niche adds further complexity and raises the possibility that different host-associated groups may occupy distinct ecological niches within Britain.

The repeated detection of *P. pseudosyringae* in symptomatic larch tissues, together with its ability to cause significant lesions on Japanese larch in inoculation trials, supports the hypothesis that it can act as a pathogen of larch. Although other *Phytophthora* species are known to infect larch, co-detection of *P. pseudosyringae* and *P. ramorum* appears infrequent. Of 1197 larch samples submitted for *Phytophthora* testing in 2025, *P. pseudosyringae* was detected in 341 samples, of which 330 (96.8%) were positive for *P. pseudosyringae* alone, and only 11 (3.2%) were positive for both *P. pseudosyringae* and *P. ramorum* (Forest Research, unpublished data). The overlapping symptomatology, host range and distribution of *P. pseudosyringae* and *P. ramorum* make diagnosis based on symptoms alone unreliable. It also

presents particular challenges for disease surveillance and management, as larch stands exhibiting symptoms consistent with *P. ramorum* infection may subsequently be found to be due to *P. pseudosyringae*. While our observations support the role of *P. pseudosyringae* in larch disease, additional studies would help clarify its contribution to larch decline under field conditions and improve understanding of its epidemiology in forest environments.

In Britain, the potential role of *P. pseudosyringae* as a primary pathogen presents regulatory and management challenges. Unlike *P. ramorum*, which is a quarantine pathogen subject to statutory control, *P. pseudosyringae* is unregulated. This regulatory discrepancy can create practical difficulties for landowners and stakeholders and political difficulties for policy makers, particularly when both Phytophthora species cause similar visible symptoms on *Larix* but lead to very different management outcomes. In this study, pathogenicity varied markedly between host-associated groups, adding to potential management difficulties. *Larix*-associated isolates consistently produced larger lesions on Japanese larch, comparable to those caused by *P. ramorum*, whereas isolates from *Vaccinium* and *Fagus-Nothofagus* produced smaller or negligible lesions. These results suggest that pathogenicity in *P. pseudosyringae* is not uniform and that disease risk may vary among host-associated groups and hosts. These findings highlight the importance of laboratory diagnosis and accurate pathogen identification when investigating larch decline, as disease symptoms alone may not reliably distinguish between *P. pseudosyringae* and *P. ramorum*, and pathogenicity may vary among host-associated groups of *P. pseudosyringae*.

This study also revealed that the impacts of *P. pseudosyringae* (based on lesion size) were greater in autumn compared to spring, which may reflect seasonal changes in host susceptibility, mediated through changes in defence compounds or bark moisture. Lesion size also decreased with height on the stem, potentially reflecting vertical gradients in cambial activity or bark structure. These spatial and temporal effects further highlight the importance of host–pathogen–environment interactions in disease expression and should be considered in host risk studies and disease modelling. While the experiments presented here provide evidence of phenotypic and pathogenic variation among the host-associated groups of *P. pseudosyringae*, they were conducted under controlled conditions. Further studies under field conditions, incorporating a broader range of isolates and host species, will be important to determine how these differences influence disease development and epidemiology in forest environments.

5. Conclusions

Taken together, our findings support the presence of genetically differentiated lineages of *P. pseudosyringae* in Britain, consistent with the population structure identified previously [22]. Genetic differentiation within the species is associated with differences in host association, morphology, growth characteristics and pathogenicity. It is unclear whether these patterns reflect local adaptation, host-associated differentiation, the introduction of divergent genotypes and recombination within the population, or other evolutionary processes. Furthermore, as host-associated groups were not evenly distributed geographically, the relative contributions of host association and geographic structure remain unresolved. Further investigation into potential host-specific adaptations, sporulation capacity, and broader host range testing will be needed to evaluate the risk posed by this species to forestry and other habitats. What is evident is that the *Larix*-associated group of *P. pseudosyringae* caused lesions on Japanese larch comparable to those produced by *P. ramorum* under the conditions tested. These findings suggest that this host-associated group has the potential to be an important pathogen of larch in the British Isles.

Supplementary Materials: The following supporting information can be downloaded at https://www.mdpi.com/article/10.3390/f17111344/s1. Supplementary Table S1. GenBank accession numbers for *Phytophthora pseudosyringae* isolates and representative ITS Clade 3 species sequenced in this study.

Author Contributions: Conceptualization, A.R.H.; methodology, A.R.H.; formal analysis, M.S.M. and A.R.H.; data curation, M.S.M.; writing—original draft preparation, A.R.H.; writing—review and editing, J.F.W. and M.S.M.; supervision, J.F.W.; funding acquisition, J.F.W. and M.S.M. All authors have read and agreed to the published version of the manuscript.

Funding: This work was predominantly funded through the Forestry Science and Innovation Strategy and partially funded by the European Regional Development Fund (Project Phytophthora Research Centre, Reg. No. CZ.02.1.01/0.0/0.0/15_003/0000453). We also thank the Phytophthora Research Centre, Mendel University, Brno, for providing three ITS Clade 3 *Phytophthora* isolates that were used as outgroup taxa in the phylogenetic analyses.

Data Availability Statement: The raw data supporting the conclusions of this article will be made available by the authors on request.

Acknowledgments: We gratefully acknowledge the invaluable assistance of Forest Research statisticians Toni Clarke and Victoria Lee in reviewing our analysis. We also thank Forest Research colleagues who, over many years, have contributed to the Phytophthora Culture Collection, which supplied the majority of isolates used in this study.

Conflicts of Interest: The authors declare no conflicts of interest. The funders had no role in the design of the study; in the collection, analyses, or interpretation of data; in the writing of the manuscript; or in the decision to publish the results.

References

1. Jung, T.; Nechwatal, J.; Cooke, D.E.L.; Hartmann, G.; Blaschke, M.; Oßwald, W.F.; Duncan, J.M.; Delatour, C. *Phytophthora pseudosyringae* sp. nov., a new species causing root and collar rot of deciduous tree species in Europe. *Mycol. Res.* **2003**, *107*, 772–789. [CrossRef]
2. Denman, S.; Rose, J.; Slippers, B. *Phytophthora pseudosyringae* Found on European Beech and Hornbeam Trees in the United Kingdom. In *Proceedings of the Fourth Meeting of the International Union of Forest Research Organizations (IUFRO) Working Party S07.02.09: Phytophthoras in Forests and Natural Ecosystems*; Goheen, E.M., Frankel, S.J., Eds.; USDA Forest Service: Albany, CA, USA, 2009; pp. 273–280.
3. Brasier, C.M.; Jung, T. Recent developments in *Phytophthora* diseases of trees and natural ecosystems in Europe. In *Progress in Research on Phytophthora Diseases of Forest Trees*; Brasier, C.M., Jung, T., Osswald, W., Eds.; Proceedings of the 3rd IUFRO Working Party S07.02.09; Forest Research: Farnham, UK, 2006.
4. Day, W.R. Root-rot of sweet chestnut and beech caused by species of *Phytophthora*. I. Cause and symptoms of disease: Its relation to soil conditions. *Forestry* **1938**, *12*, 101–116.
5. Beales, P.A.; Giltrap, P.M.; Webb, K.M.; Ozolina, A. A further threat to UK heathland bilberry (*Vaccinium myrtillus*) by *Phytophthora pseudosyringae*. *Plant Pathol.* **2010**, *59*, 406. [CrossRef]
6. Bregant, C.; Rossetto, G.; Meli, L.; Sasso, N.; Montecchio, L.; Brglez, A.; Piškur, B.; Ogris, N.; Maddau, L.; Linaldeddu, B.T. Diversity of *Phytophthora* species involved in new diseases of mountain vegetation in Europe with the description of *Phytophthora pseudogregata* sp. nov. *Forests* **2023**, *14*, 1515. [CrossRef]
7. Bregant, C.; Batista, E.; Hilario, S.; Linaldeddu, B.T.; Alves, A. Diversity and Distribution of *Phytophthora* Species Along an Elevation Gradient in Natural and Semi-Natural Forest Ecosystems in Portugal. *Pathogens* **2025**, *14*, 103. [CrossRef]
8. Černý, K. Nepůvodní invazní patogeny dřevin—Výzva, nebo předem ztracený boj? *Živa* **2016**, *6*, 286–291.
9. Christova, P.K.; Lyubenova, A.B.; Kostov, K.V.; Slavov, S.B. First report of *Phytophthora pseudosyringae* re-covered from aquatic ecosystems in Bulgaria. *For. Pathol.* **2019**, *49*, e12505. [CrossRef]
10. Motta, E.; Annesi, T.; Pane, A.; Cooke, D.E.L.; Cacciola, S.O. A new *Phytophthora* sp. causing a basal canker on beech in Italy. *Plant Dis.* **2003**, *87*, 1005. [CrossRef]
11. O'Hanlon, R.; McCracken, A.R.; Cooke, L.R. Diversity and ecology of *Phytophthora* species on the Island of Ireland. *Biol. Environ.* **2016**, *116B*, 27–51. [CrossRef]
12. Redondo, M.Á.; Boberg, J.; Stenlid, J.; Oliva, J. First report of *Phytophthora pseudosyringae* causing basal cankers on horse chestnut in Sweden. *Plant Dis.* **2016**, *100*, 1024. [CrossRef]

13. Ruffner, B.; Rigling, D.; Schoebel, C.N. Multispecies *Phytophthora* disease patterns in declining beech stands. *For. Pathol.* **2019**, *49*, e12514. [CrossRef]
14. Scanu, B.; Webber, J.F. Dieback and mortality of *Nothofagus* in Britain: Ecology, pathogenicity and sporulation potential of the causal agent *Phytophthora pseudosyringae*. *Plant Pathol.* **2016**, *65*, 26–36. [CrossRef]
15. Talgø, V.; Herrero, M.L.; Sundbye, A.; Brurberg, M.B.; Kitchingman, L.; Telfer, K.; Strømeng, G.M. *Phytophthora* spp. en trussel mot blåbær i Skandinavia? *Bioforsk* **2013**, *8*, 4.
16. Trzewik, A.; Orlikowski, L.B.; Oszako, T.; Nowakowska, J.A.; Orlikowska, T. The characterization of *Phytophthora* isolates obtained from diseased *Alnus glutinosa* in Poland. *Balt. For.* **2015**, *21*, 44–50.
17. Wickland, A.C.; Jensen, C.E.; Rizzo, D.M. Geographic distribution, disease symptoms and pathogenicity of *Phytophthora nemorosa* and *Phytophthora pseudosyringae* in California, USA. *For. Pathol.* **2008**, *38*, 288–298. [CrossRef]
18. Hansen, E.M.; Reeser, P.W.; Sutton, W. Ecology and pathology of *Phytophthora* ITS clade 3 species in forests in western Oregon, USA. *Mycologia* **2017**, *109*, 100–114. [CrossRef]
19. Feau, N.; McDonald, M.; Van Der Meer, B.; Zhang, Y.; Herath, P.; Hamelin, R.C. *Phytophthora* species associated with red alder dieback in British Columbia, Canada. *Can. J. Plant Pathol.* **2022**, *44*, 549–558. [CrossRef]
20. Fajardo, S.N.; Valenzuela, S.; Dos Santos, A.F.; González, M.P.; Sanfuentes, E.A. *Phytophthora pseudosyringae* associated with the mortality of *Nothofagus obliqua* in a pure stand in central-southern Chile. *For. Pathol.* **2017**, *47*, e12361. [CrossRef]
21. González, M.; Mizubuti, E.; Gonzalez, G.; Sanfuentes, E. Uncovering the hidden hosts: Identifying inoculum reservoirs for *Phytiptophthora pseudosyringae* in *Nothofagus* forests in Chile. *Plant Pathol.* **2024**, *73*, 937–947. [CrossRef]
22. Mullett, M.S.; Harris, A.R.; Scanu, B.; Van Poucke, K.; LeBoldus, J.; Stamm, E.; Bourret, T.B.; Christova, P.K.; Oliva, J.; Redondo, M.Á.; et al. Phylogeography, origin and population structure of the self-fertile emerging plant pathogen *Phytophthora pseudosyringae*. *Mol. Plant Pathol.* **2024**, *25*, e13450. [CrossRef]
23. Harris, A.; Webber, J. *Understanding the Threat Phytophthora pseudosyringae Poses to UK Forestry and the Wider Environment*; Final Report to Future Proofing Plant Health; Project Reference TH12426FR15; Forest Research: Farnham, UK, 2026.
24. Brasier, C.; Webber, J. Sudden larch death. *Nature* **2010**, *466*, 824–825. [CrossRef]
25. Brasier, C.M.; Kirk, S.A. Production of gametangia by *Phytophthora ramorum* in vitro. *Mycol. Res.* **2004**, *108*, 823–827. [CrossRef]
26. Blair, J.E.; Coffey, M.D.; Park, S.Y.; Geiser, D.M.; Kang, S. A multi-locus phylogeny for *Phytophthora* utilizing markers derived from complete genome sequences. *Fungal Genet. Biol.* **2008**, *45*, 266–277. [CrossRef]
27. Kroon, L.P.N.M.; Bakker, F.T.; van den Bosch, G.B.M.; Bonants, P.J.M.; Flier, W.G. Phylogenetic analysis of *Phytophthora* species based on mitochondrial and nuclear DNA sequences. *Fungal Genet. Biol.* **2004**, *41*, 766–782. [CrossRef]
28. Grünwald, N.J.; Martin, F.N.; Larsen, M.M.; Sullivan Press, C.M.; Coffey, M.D.; Hansen, E.M.; Parke, J.L. *Phytophthora*-ID.org: A sequence-based *Phytophthora identification* tool. *Plant Dis.* **2011**, *95*, 337–342. [CrossRef]
29. Robideau, G.P.; De Cock, A.W.A.M.; Coffey, M.D.; Voglmayr, H.; Brouwer, H.; Bala, K.; Chitty, D.W.; Désaulniers, N.; Eggertson, Q.A.; Gachon, C.M.M.; et al. DNA barcoding of oomycetes with cytochrome c oxidase subunit I and internal transcribed spacer. *Mol. Ecol. Resour.* **2011**, *11*, 1002–1011. [CrossRef]
30. Choi, Y.-J.; Beakes, G.; Glockling, S.; Kruse, J.; Nam, B.; Nigrelli, L.; Ploch, S.; Shin, H.-D.; Shivas, R.G.; Telle, S.; et al. Towards a universal barcode of oomycetes—A comparison of the *cox*1 and *cox*2 loci. *Mol. Ecol. Resour.* **2015**, *15*, 1275–1288. [CrossRef]
31. Lanfear, R.; Frandsen, P.B.; Wright, A.M.; Senfeld, T.; Calcott, B. PartitionFinder 2: New methods for selecting partitioned models of evolution for molecular and morphological phylogenetic analyses. *Mol. Biol. Evol.* **2017**, *34*, 772–773. [CrossRef]
32. Kozlov, A.M.; Darriba, D.; Flouri, T.; Morel, B.; Stamatakis, A. RAxML-NG: A fast, scalable and user-friendly tool for maximum likelihood phylogenetic inference. *Bioinformatics* **2019**, *35*, 4453–4455. [CrossRef]
33. Pattengale, N.D.; Alipour, M.; Bininda-Emonds, O.R.; Moret, B.M.; Stamatakis, A. How many bootstrap replicates are necessary? *J. Comput. Biol.* **2010**, *17*, 337–354. [CrossRef]
34. Bouckaert, R.; Heled, J.; Kühnert, D.; Vaughan, T.; Wu, C.H.; Xie, D.; Suchard, M.A.; Rambaut, A.; Drummond, A.J. BEAST 2: A software platform for Bayesian evolutionary analysis. *PLoS Comput. Biol.* **2014**, *10*, e1003537. [CrossRef]
35. Drummond, A.J.; Ho, S.Y.W.; Phillips, M.J.; Rambaut, A. Relaxed phylogenetics and dating with confidence. *PLoS Biol.* **2006**, *4*, e88. [CrossRef]
36. Rambaut, A.; Drummond, A.J.; Xie, D.; Baele, G.; Suchard, M.A. Posterior summarization in Bayesian phylogenetics using Tracer 1.7. *Syst. Biol.* **2018**, *67*, 901–904. [CrossRef]
37. Stöver, B.C.; Müller, K.F. TreeGraph 2: Combining and visualizing evidence from different phylogenetic analyses. *BMC Bioinform.* **2010**, *11*, 7. [CrossRef]
38. R Core Team. *R: A Language and Environment for Statistical Computing*; R Foundation for Statistical Computing: Vienna, Austria, 2018.
39. Bates, D.; Maechler, M.; Bolker, B.; Walker, S. Fitting Linear Mixed-Effects Models Using lme4. *J. Stat. Softw.* **2015**, *67*, 1–48. [CrossRef]

40. Lenth, R. *Emmeans: Estimated Marginal Means, aka Least-Squares Means, R package version 1.10.5*; R Foundation for Statistical Computing: Vienna, Austria, 2024.
41. Franceschini, S.; Webber, J.F.; Sancisi-Frey, S.; Brasier, C.M. Gene × Environment tests discriminate the new EU2 evolutionary lineage of *Phytophthora ramorum* and indicate it is adaptively different. *For. Pathol.* **2014**, *44*, 219–232. [CrossRef]
42. Tuite, J. *Plant Pathological Methods: Fungi and Bacteria*; Burgess Publishing Company: Minneapolis, MN, USA, 1969.
43. Strong, R.A.; Kolodny, E.; Kelsey, R.G.; Gonzalez-Hernandez, M.P.; Vivanco, J.M.; Manter, D.K. Effect of plant sterols and tannins on *Phytophthora ramorum* growth and sporulation. *J. Chem. Ecol.* **2013**, *39*, 733–743. [CrossRef]
44. Harris, A.R.; Webber, J.F. Insights into the potential host range of *Phytophthora foliorum*. *For. Pathol.* **2019**, *49*, e12556. [CrossRef]
45. Harris, A.R.; Brasier, C.M.; Scanu, B.; Webber, J.F. Fitness characteristics of the European lineages of *Phytophthora ramorum*. *Plant Pathol.* **2021**, *70*, 275–286. [CrossRef]
46. Schneider, C.A.; Rasband, W.S.; Eliceiri, K.W. NIH Image to ImageJ: 25 years of image analysis. *Nat. Methods* **2012**, *9*, 671–675. [CrossRef]
47. Brasier, C.M.; Beales, P.A.; Kirk, S.A.; Denman, S.; Rose, J. *Phytophthora kernoviae* sp. nov., an invasive pathogen causing bleeding stem lesions on forest trees and foliar necrosis of ornamentals in Britain. *Mycol. Res.* **2005**, *109*, 853–859. [CrossRef]
48. R Core Team. *R: A Language and Environment for Statistical Computing*; R Foundation for Statistical Computing: Vienna, Austria, 2024.
49. Kuznetsova, A.; Brockhoff, P.B.; Christensen, R.H.B. lmerTest Package: Tests in Linear Mixed Effects Models. *J. Stat. Softw.* **2017**, *82*, 1–26. [CrossRef]
50. Scanu, B.; Linaldeddu, B.T.; Peréz-Sierra, A.; Deidda, A.; Franceschini, A. *Phytophthora ilicis* as a leaf and stem pathogen of *Ilex aquifolium* in Mediterranean islands. *Phytopathol. Mediterr.* **2014**, *53*, 480–490. [CrossRef]
51. Mullett, M.S.; Van Poucke, K.; Haegeman, A.; Focquet, F.; Cauldron, N.; Knaus, B.; Horta Jung, M.; Kageyama, K.; Hieno, A.; Masuja, H.; et al. Phylogeography and population structure of the global, wide host-range hybrid pathogen *Phytophthora* × *cambivora*. *IMA Fungus* **2023**, *14*, 4. [CrossRef]

Disclaimer/Publisher's Note: The statements, opinions and data contained in all publications are solely those of the individual author(s) and contributor(s) and not of MDPI and/or the editor(s). MDPI and/or the editor(s) disclaim responsibility for any injury to people or property resulting from any ideas, methods, instructions or products referred to in the content.